Comparative study of electroabsorption in InGaN/GaN quantum zigzag heterostructures with polarization-induced electric fields

Emre Sari, Tuncay Ozel, Aslı Koc, Jin-Woo Ju, Haeng-Keun Ahn et al.

Citation: Appl. Phys. Lett. **92**, 201105 (2008); doi: 10.1063/1.2931696
View online: http://dx.doi.org/10.1063/1.2931696
View Table of Contents: http://apl.aip.org/resource/1/APPLAB/v92/i20
Published by the American Institute of Physics.

Comparative study of electroabsorption in InGaN/GaN quantum zigzag heterostructures with polarization-induced electric fields

Emre Sari,[1,2,3] Tuncay Ozel,[2,3,4] Aslı Koc,[2,3] Jin-Woo Ju,[5] Haeng-Keun Ahn,[5] In-Hwan Lee,[5] Jong-Hyeob Baek,[6] and Hilmi Volkan Demir[1,2,3,4,a)]

[1]*Department of Electrical and Electronics Engineering, Bilkent University, Ankara TR-06800 Bilkent, Turkey*

[2]*Nanotechnology Research Center, Bilkent University, Ankara TR-06800 Bilkent, Turkey*

[3]*Institute of Materials Science and Nanotechnology, Bilkent University, Ankara TR-06800 Bilkent, Turkey*

[4]*Department of Physics, Bilkent University, Ankara TR-06800 Bilkent, Turkey*

[5]*School of Advanced Materials Engineering, Research Center of Industrial Technology, Chonbuk National University, Chonju 561-756, Republic of Korea*

[6]*Korea Photonics Technology Institute, Gwangju 500-460, Republic of Korea*

(Received 2 April 2008; accepted 29 April 2008; published online 19 May 2008)

We present a comparative study on InGaN/GaN quantum zigzag structures embedded in *p-i-n* diode architecture that exhibit blue-shifting electroabsorption in the blue when an electric field is externally applied to compensate for the polarization-induced electric field across the wells. With the polarization breaking their symmetry, the same InGaN/GaN quantum structures redshift their absorption edge when the external field is applied in the same direction as the well polarization. Both computationally and experimentally, we investigate the effects of polarization on electroabsorption by varying compositional content and structural parameters and demonstrate that electroabsorption grows stronger with weaker polarization in these multiple quantum well modulators. © *2008 American Institute of Physics*. [DOI: 10.1063/1.2931696]

An important, distinctive property of III-nitride quantum heterostructures is the formation of strong polarization when they are grown on the *c* plane of their wurtzite crystal structure.[1] Due to the discontinuity of polarization with abrupt compositional changes at the heterointerfaces of such III-N multiple quantum wells (MQWs), large electrostatic fields in alternating directions are induced across the well/barrier pairs. As a result, the band structure of these MQWs yields zigzag potential profiles in conduction and valence bands instead of conventional square potential profiles. This substantially alters electric field dependence of optical absorption in III-N MQW structures.

Electroabsorption measurements are also essentially informative to understand the underlying physics behind such polar III-N structures. We previously demonstrated a quantum electroabsorption modulator based on InGaN/GaN quantum zigzag structures operating in the blue[2] and in the near-ultraviolet.[3] In the previous work of our group and others, however, the effect of polarization on electroabsorption in polar InGaN/GaN has not been comparatively studied or systematically investigated to date.[2–4] To this end, in this letter, we present the design, growth, fabrication, experimental characterization, and theoretical analysis of InGaN/GaN quantum zigzag structures with different levels of polarization-induced electrostatic fields that are set by controlling the alloy content and well-to-barrier width ratio. In this work, we comparatively study the effects of polarization-induced electrostatic field on the performance of our quantum electroabsorption modulators and develop a better understanding to design devices for stronger electroabsorption.

Polarization in III-nitrides consists of piezoelectric and spontaneous components. The discontinuity of the total polarization causes accumulation of very high density ($\sim 10^{13}$ cm^{-2}), two-dimensional electron gas (2DEG) and 2D hole gas (2DHG) at the heterointerfaces.[5] Moreover, in MQW structures, the alternating sign of 2D charge densities in the well-to-barrier and barrier-to-well heterointerfaces results in built-in electrostatic fields that also alternate in direction.[1] These polarization-induced built-in electrostatic fields across the wells and the barriers are expressed in Eqs. (1) and (2), respectively, such that there is no voltage build up across the whole MQW structure. Here, spontaneous and piezoelectric polarization for any periodic MQW structure formed in InAlGaN alloys can be calculated using the material parameters of InN, AlN, and GaN with a first order interpolation. As evident from Eqs. (1) and (2), besides the well and barrier alloy content, the built-in electrostatic field depends on the well-to-barrier width ratio.

$$\mathbf{E}_{\mathrm{tot}}^{\mathrm{well}} = \mathbf{E}_{\mathrm{sp}}^{\mathrm{well}} + \mathbf{E}_{\mathrm{pz}}^{\mathrm{well}} = \frac{(\mathbf{P}_{\mathrm{sp}}^{\mathrm{barrier}} + \mathbf{P}_{\mathrm{pz}}^{\mathrm{barrier}}) - (\mathbf{P}_{\mathrm{sp}}^{\mathrm{well}} + \mathbf{P}_{\mathrm{pz}}^{\mathrm{well}})}{\epsilon_{\mathrm{well}} + \frac{d_{\mathrm{well}}}{d_{\mathrm{barrier}}}\epsilon_{\mathrm{barrier}}}. \tag{1}$$

$$\mathbf{E}_{\mathrm{tot}}^{\mathrm{barrier}} = \mathbf{E}_{\mathrm{sp}}^{\mathrm{barrier}} + \mathbf{E}_{\mathrm{pz}}^{\mathrm{barrier}} = \frac{(\mathbf{P}_{\mathrm{sp}}^{\mathrm{well}} + \mathbf{P}_{\mathrm{pz}}^{\mathrm{well}}) - (\mathbf{P}_{\mathrm{sp}}^{\mathrm{barrier}} + \mathbf{P}_{\mathrm{pz}}^{\mathrm{barrier}})}{\epsilon_{\mathrm{barrier}} + \frac{d_{\mathrm{barrier}}}{d_{\mathrm{well}}}\epsilon_{\mathrm{well}}}. \tag{2}$$

For our comparative study, we designed three sets of InGaN/GaN quantum structures incorporated in a *p-i-n* diode architecture. Among these sets, the structural parameters of their active regions were carefully selected for comparison purposes. These structural parameters include InN concentra-

a)Author to whom correspondence should be addressed. Electronic mail: volkan@bilkent.edu.tr. Tel.: [+90](312) 290-1021. FAX: [+90](312) 290-1015.

tions in the quantum well regions and well-to-barrier width ratios. We used a generic *p-i-n* epitaxial design for these three sets of samples (samples *A*, *B*, and *C*). In our design, we included five quantum well/barrier pairs for all of the structures. Sample *A* was designed to have an active MQW layer of 2.5 nm/7.5 nm $In_{0.15}Ga_{0.85}N/GaN$ quantum well/barrier structures. Sample *B* has the same structure with 3 nm/4 nm $In_{0.15}Ga_{0.85}N/GaN$ and Sample *C* with 3 nm/4 nm $In_{0.12}Ga_{0.88}N/GaN$. These epistructures were designed to study only the polarization effect varied through these two parameters. Using the design and material parameters of GaN and InN, we calculate built-in electrostatic fields inside the well and barrier layers of samples *A*, *B*, and *C*. The polarization-induced electric field across the wells were set to be −383 V/μm for sample *A*, −300 V/μm for sample *B*, and −238 V/μm for sample *C*, while those across the barriers were set to be 127 V/μm for sample *A*, 220 V/μm for sample *B*, and 179 V/μm for sample *C*.

We grew these epitaxial structures using a metal organic chemical vapor deposition system on *c*-plane sapphire substrates. We used exactly the same conditions for the epitaxial growth of all samples except for their active layers. We tuned InN incorporation into the MQW layers by changing the growth temperature and their layer thickness by changing the growth time of each layer. Detailed growth conditions can be found elsewhere.[6] Following the epitaxial growth, we fabricated diode mesas with electrodes using reactive ion etching, *p* and *n* contact metallization, and annealing steps.[2,3] The three samples in this work were all fabricated using our standard semiconductor processes[7–9] and then characterized under the same conditions. We performed photoluminescence (PL) and double crystal x-ray diffraction (DCXRD) measurements to verify the growth of the desired quantum structures with the intended alloy content and high crystal quality. PL spectra for these samples were obtained using a He–Cd laser at an excitation wavelength of 325 nm. PL peaks at 450, 450, and 425 nm for samples *A*, *B*, and *C*, respectively, verify the growth of the InGaN quantum wells within 1.5% of the desired InN ratio.

Figure 1 shows a typical PL spectrum and electroluminescence spectrum from an exemplary sample (sample *C*). Also in the inset of the same figure, we present a micrograph of the fabricated device under forward bias. The PL characteristics with a tail at longer wavelengths hint at the phase separation. The DCXRD spectra, also shown in the inset of Fig. 1, verifies the growth of MQW structures with a desired periodicity (well+barrier thickness) of 10.0, 7.2, and 7.1 nm for samples *A*, *B*, and *C*, respectively.

Together with the experimental verification of the structural parameters and the calculated built-in electrostatic fields, we obtained full band diagram of the grown InGaN/GaN quantum zigzag structures, with a potential profile[1,2] tilting in one direction in the wells and in the other direction in the barriers. We developed a transfer matrix method for the numerical analysis of these quantum structures. Using our computational tool, we computed ground state electron and heavy hole eigenstates and eigenenergies along with the squared overlap integral of $|\langle e_1|h_1\rangle|^2$ proportional to the absorption strength under different levels of external electric field. Traditional quantum confined Stark effect yields only red shift, independent of the direction of the applied electric field.[10] For all of our samples (samples *A*, *B*, and *C*) with the increasing external electric field, when it is applied in the opposite direction of the polarization-induced electric field across the wells, we computationally prove that the absorption edge blueshifts. In this case, the external field compensates for the internal field in the wells. However, when the external field is applied in the same direction as the polarization in the wells, the same InGaN/GaN quantum structures redshift their absorption edge. The co-observation of these blue and red shifts in the electroabsorption of the same quantum structures is impossible in nonpolar quantum heterostructures, which are completely indifferent to the direction of the applied field. In the case of such polar III-N quantum heterostructures, the polarization breaks their symmetry and thus, the direction of the applied field matters. Our theoretical results predict absorption coefficient changes with the ratios of 0.4 around $\lambda=450$ nm for sample *A*, 0.53 around $\lambda=440$ nm for sample *B*, and 1.0 around $\lambda=420$ nm for sample *C* with a field swing of 40 V/μm. Therefore, sample *C*, which features the weakest polarization, is theoretically predicted to exhibit the strongest electroabsorption.

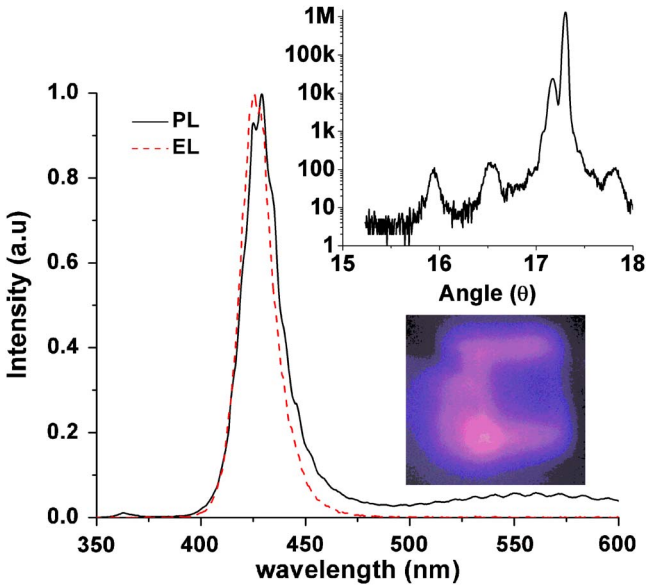

FIG. 1. (Color online) PL and electroluminescence spectra obtained from an exemplary InGaN/GaN quantum structure (sample *C*). Inset shows the DCXRD spectrum along with a micrograph of its electroluminescence.

In electroabsorption measurements, by chopping the incident optical beam and monitoring the photocurrent with a lock-in amplifier at the chopping frequency, we observe a blue shift of the absorption edge with the application of reverse bias, which generates an electric field opposite to the polarization in the wells. Figures 2–4 show optical absorption spectra around the corresponding operating wavelengths for each of the sample (samples *A*, *B*, and *C*, respectively). Additionally, in insets (a) of Figs. 2–4, we present the absorption coefficient change with respect to the 0 V absorption curve for each sample. Our analysis of absorption coefficient change reveals that we obtain a maximum absorption coefficient change of 288 cm^{-1} at $\lambda=440$ nm for sample *A*, 462 cm^{-1} at $\lambda=434$ nm for sample *B*, and 555 cm^{-1} at $\lambda=422$ nm for sample *C*, which are all obtained by a 0–4 V swing (for a field change of 40 V/μm). These correspond to the relative ratios of 0.52 at 440 nm for sample *A*, 0.83 at 434 nm for sample *B*, and 1.0 at 422 nm for sample *C*. These experimental results are in good agreement with our compu-

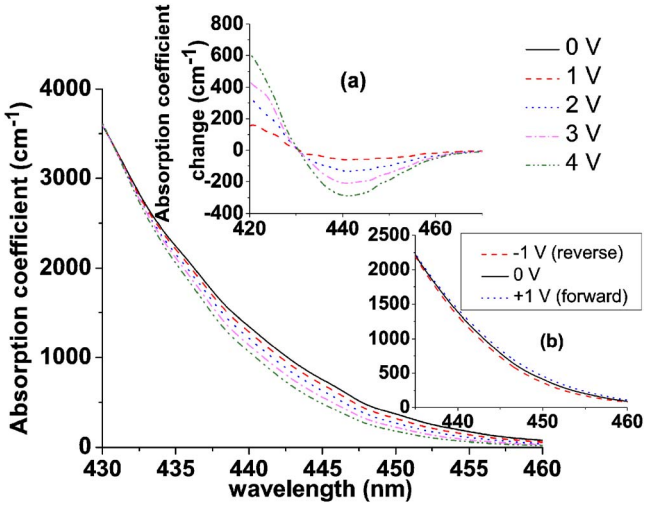

FIG. 2. (Color online) Electroabsorption spectra of sample *A* under different bias voltages. The inset (a) shows the absorption coefficient change for sample *A* with respect to the 0 V absorption curve and the inset (b) depicts the absorption spectra of sample *A* for 0, −1, and +1 V bias voltages.

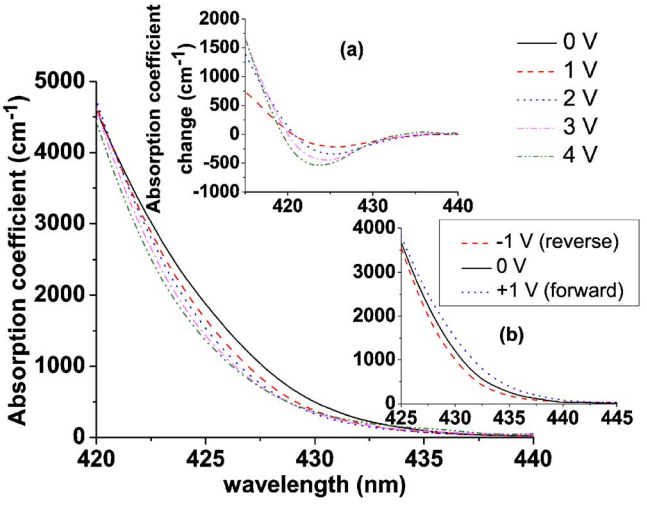

FIG. 4. (Color online) Electroabsorption spectra of sample *C* under different bias voltages. The inset (a) shows the absorption coefficient change for sample *C* with respect to the 0 V absorption curve and the inset (b) depicts the absorption spectra of sample *C* for 0, −1, and +1 V bias voltages.

tational results. Experimentally, sample *C*, which has the weakest polarization, exhibits the largest absorption change, which is like the theoretical prediction. The electroabsorption improves with decreasing built-in electrostatic field inside the wells. Additionally, insets (b) of the respective electroabsorption figures of samples *A*–*C* (Figs. 2–4) also present the absorption curves under 0 V, −1 V (in reverse bias), and 1 V (in forward bias). While the current levels in the forward bias at 1 V and in the reverse bias at −1 V are similar, the electric field generated at 1 V and −1 V is completely opposite in direction. This change in the electric field direction then reverses the shift of the absorption edge from blue shift to red shift. This behavior is unique to polar quantum heterostructures, which is both predicted by our theoretical computations and verified by our experimental characterization.

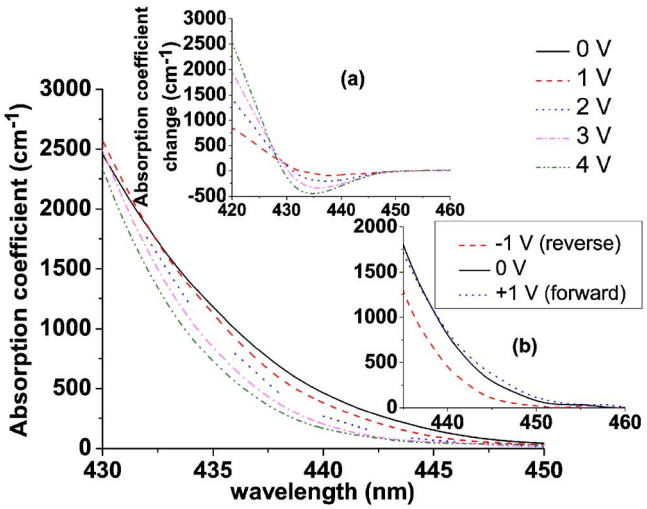

FIG. 3. (Color online) Electroabsorption spectra of sample *B* under different bias voltages. The inset (a) shows the absorption coefficient change for sample *B* with respect to the 0 V absorption curve and the inset (b) depicts the absorption spectra of sample *B* for 0, −1, and +1 V bias voltages.

In conclusion, we conducted a comparative study of electroabsorption in polar InGaN/GaN quantum structures with different InN ratios and well-to-barrier widths. These quantum zigzag structures exhibit blue-shifting electroabsorption when an electric field is externally applied in the opposite direction of the polarization across the wells of the zigzag structures. The same quantum structures redshift their absorption edge when the external field is applied in the same direction as the polarization in the wells. Both computationally and experimentally, we conclude that electroabsorption grows stronger with weaker polarization.

This work is supported by EU-PHOREMOST NoE 511616 and Marie Curie IRG MOON 021391 and TUBITAK EEEAG 104E114, 107E297, 107E080, 106E020, 105E065, and 105E066. Also, H.V.D. acknowledges additional support from the Turkish Academy of Sciences Distinguished Young Scientist Award (TUBA GEBIP) and European Science Foundation (ESF) European Young Investigator Award (EURYI) Programs.

[1] V. Fiorentini, F. Bernardini, F. D. Sala, A. Di Carlo, and P. Lugli, Phys. Rev. B **60**, 8849 (1999).
[2] E. Sari, T. Ozel, S. Nizamoglu, and H. V. Demir, Appl. Phys. Lett. **90**, 011101 (2007).
[3] T. Ozel, E. Sari, S. Nizamoglu, and H. V. Demir, J. Appl. Phys. **102**, 113101 (2007).
[4] I. Friel, C. Thomidis, and T. D. Moustakas, J. Appl. Phys. **97**, 123515 (2005).
[5] N. Maeda, T. Saitoh, K. Tsubaki, T. Nishida, and N. Kobayashi, Phys. Status Solidi A **216**, 727 (1999).
[6] J. W. Ju, C. R. Lee, J. H. Baek, Y. H. Lee, and I. H. Lee, Jpn. J. Appl. Phys., Part 1 **44**, 2506 (2005).
[7] S. Nizamoglu and H. V. Demir, Nanotechnology **18**, 405702 (2007).
[8] H. V. Demir, V. A. Sabnis, O. Fidaner, J. S. Harris, Jr., D. A. B. Miller, and J.-F. Zheng, Opt. Express **12**, 310 (2004).
[9] S. Nizamoglu and H. V. Demir, J. Opt. A, Pure Appl. Opt. **9**, S419 (2007).
[10] D. A. B. Miller, D. S. Chemla, T. C. Damen, A. C. Gossard, W. Wiegmann, T. H. Wood, and C. A. Burrus, Phys. Rev. B **32**, 1043 (1985).